ELSEVIER

Journal of Hazardous Materials A124 (2005) 1–18

Journal of Hazardous Materials

www.elsevier.com/locate/jhazmat

Toxic gas clouds: Effects and implications of dry deposition on concentration

Lage Jonsson *, Edvard Karlsson, Lennart Thaning

FOI, Swedish Defence Research Agency, Division of NBC Defence, SE-901 82 Umeå, Sweden

Received 28 October 2003; received in revised form 15 April 2005; accepted 16 April 2005
Available online 9 June 2005

Abstract

The influence of the dry deposition process on concentration pertaining to toxic gas clouds was investigated by model calculations. Three main release scenarios were simulated, with nine micrometeorological cases considered for each. To compare and confirm the results, two model types, a stochastic particle model and a box-type model, were independently used to simulate many of the different cases. The results showed that the effects of dry deposition may be strong for releases at, or confined close to the ground, e.g. neutral or unstable stratification can cause higher concentrations than stable stratification after 10–15 km. Risk distances are in turn affected and may be substantially shortened, e.g. for a zero-height release like that from an evaporating pool, a 50% reduction in total airborne substance may occur within 500 m at a low wind velocity and neutral or stable stratification.
© 2005 Elsevier B.V. All rights reserved.

Keywords: Dry deposition; Toxic gas clouds; Stochastic particle model; Risk distance; Box model

1. Introduction

The aim of this research was to call attention to some of the effects of dry deposition on concentration regarding hazardous gas clouds and in particular to the importance of the combined effect of dry deposition and atmospheric stratification as well as release height. The investigation used SO_2 and the nerve agents sarin and VX as examples of hazardous gases.

The processes of dry deposition and wet deposition control the amount of pollutant that is transferred to a surface. Dry deposition influences the concentration of the pollutant in the air and its residence time. It is usually formulated in dispersion models by using the dry deposition velocity, v_d, defined as $v_d = F/C$, where F is the flux to the surface and C is the concentration of an agent at some reference height. Reactive or water miscible/soluble gases often have a higher v_d than non-reactive or immiscible gases. A dry deposition velocity in the range of 1.6–3.7 cm s^{-1} has been reported in literature for Cl_2 and HF and a dry deposition velocity of 0.04–7.5 cm s^{-1} for SO_2 [1]. The SO_2 values are from 14 different published measurements made under various conditions. The lowest value (0.04) represents a laboratory measurement. A value of 0.05 is for snow under stable conditions. The highest value (7.5) corresponds to urban conditions (St. Louis). The nerve agents sarin and VX, which are highly soluble in water, have an estimated dry deposition velocity of approximately 0.5 and 2 cm s^{-1}, respectively, under summer conditions but lower values in wintertime [2].

Normally, calculation of the removal of gaseous toxic substances from the air by dry deposition is included in regional-scale dispersion models used in air-quality and environmental studies [3–5]. However, in some models dry deposition has not been applied in the near field [3] since it is assumed more important at greater downwind distances. Dry deposition is a process also included in some hazardous-gas dispersion models, for example HGSYSTEM [6]. Hazardous-gas models also exist which exclude dry deposition without explanation [7–8], a possible indication that the effect of dry deposition may be underestimated. Heavy-gas and hazardous-gas dispersion models designed only for short distances often do

* Corresponding author. Tel.: +46 90 10 68 36; fax: +46 90 10 68 02.
E-mail address: lage.jonsson@foi.se (L. Jonsson).

0304-3894/$ – see front matter © 2005 Elsevier B.V. All rights reserved.
doi:10.1016/j.jhazmat.2005.04.018

not take dry deposition into account because it is believed to be of minor significance compared to other factors [9–12]. When v_d is taken into account in hazardous-gas dispersion models, it is normally treated as a constant or a near constant. In models of air quality, v_d is often a function of time of day and year, terrain and weather, and furthermore, v_d is calculated from aerodynamic resistance, viscous sub-layer resistance and surface resistance [4].

Observations made from a chlorine accident along with supportive experiments [13], point to absorption of 1000 kg of chlorine within a 500 m radius from a chlorine release of 5000 kg. The wind speed was 1–1.5 m s^{-1} and the dispersion was slow due to an uneven terrain. This accident indicates a need to include dry deposition in the near-field modeling of the dispersion of hazardous gases. Singh and Ghosh [14] found it very important to consider dry deposition in modeling the dispersion of the methyl isocyanate in the Bhopal gas tragedy. They found that dry deposition and chemical reactions with atmospheric moisture significantly reduced the residence time of the gas and the affected area. Without these processes, the event would have been far more tragic than it was. Dry deposition has also been shown to be capable of significantly reducing the indoor concentration of toxic gases released outdoors [15–16] especially at low ventilation rates.

In their *Handbook on Atmospheric Dispersion,* Hanna et al. [17] present Gaussian model calculations, which show that the largest transfers of substance to the surface occur when the release is at the surface, the atmospheric stratification is very stable and the wind speed is low. As much as 50% of the released substance could be transferred to the surface within 100 m. The transfer to the surface is lower in neutral and unstable stratification, or if the release is placed at some height above the surface. Karlsson [18] showed that a high mixing height (i.e. unstable stratification) is most favorable for the long-range transport of pollutants due to low deposition with model calculations using a simple box model. A rough estimation showed that the residence time for a pollutant in the atmosphere is proportional to H/v_d, where H is the mixing height of the boundary layer and v_d is the dry deposition velocity. Thus, the longest residence times and most favorable conditions for long-range transport are achieved at unstable stratification when H is largest despite the fact that the increased dispersion works in the other direction.

The discussion above raises a question: can the large dry deposition transfer to the surface in stable stratification, shown by Hanna et al., influence the concentration from a ground-level release in such a way that the highest concentration is achieved not in stable stratification, but instead in neutral or unstable stratification? If the answer were to be yes, this would be contrary to what is normally believed and to views reflected in many rules of thumb and handbooks [8,19,20]. If not, will the concentration from a ground-level release at a short distance be highest at a stable concentration, but for a longer distance shift to being highest at neutral or unstable stratification and, if so, at which distance would this shift occur? Other questions to be addressed are how release height influences the effects of dry deposition and whether or not calculations using more sophisticated models will render similar results to previous calculations with Gaussian and box models that use a constant v_d value.

In this study three models, a Lagrangian dispersion model [21], a long-range transport box model [18] and a puff box model, were employed to show some of the effects of dry deposition on the concentration of hazardous gas clouds and the importance of release height and atmospheric stratification. Simulations of three different release scenarios occurring under different weather conditions were carried out with each model and the results compared.

2. Dry deposition modeling

The dry deposition flux of gases and particles from the atmosphere to the surface is governed by their concentration in the air, turbulent transport in the boundary layer, molecular transport in the viscous sub-layer and by the chemical and physical nature of the depositing species that determine how efficiently the surface can capture or absorb gases and particles. To describe the exchange process three stages are commonly identified working in series like three resistances, a resistance analogy [22–23]. This provides a common framework for the parameterization of the deposition velocity, defined by the relation [24]:

$$F = v_d(z_{ref})C(z_{ref}) \tag{1}$$

where z_{ref} is a reference height, F is the flux of species to the surface, $C(z_{ref})$ is the concentration at height z_{ref} and v_d is the dry deposition velocity. Within this framework, v_d provides a measure of conductivity between atmosphere and ground and is as such widely used to parameterize gas uptake on the ground [25–27], according to:

$$v_d = \frac{1}{R_a + R_s + R_c} \tag{2}$$

where R_a is the aerodynamic resistance in the atmospheric surface layer [28], R_s is the sub-layer resistance [29], and R_c is the surface (canopy) resistance [30].

$$R_a = \frac{(\ln(z_{ref}/z_0) - \Psi(z_{ref}/L))}{\kappa u_*} \tag{3}$$

where z_0 is the roughness height, Ψ the integrated stability function for momentum [28], L the Monin-Obukhov length, κ is von Karman constant, u_* is the friction velocity and z_{ref} is the reference height, which in the case of the box model is half the vertical extent of the cloud. The variable u_* in the box-type models used in this investigation (Section 3) is determined by:

$$u_* = \frac{\kappa u}{(\ln(z_{ref}/z_0) - \Psi(z_{ref}/z_0))} \tag{4}$$

where u is the wind speed.

R_s is calculated by:

$$R_s = \frac{2(\nu_{air}/D_{substance})^{2/3}}{\kappa \times u_*} \quad (5)$$

where ν_{air} is the kinematic viscosity of air and $D_{substance}$ denotes the molecular diffusivity of the substance in air. It is worth noting that different researchers recommend different expressions for R_s. For example, some use an expression where they divide the Schmidt number ($\nu_{air}/D_{substance}$) by the Prandtl number (which is assumed to be 0.72) [31], [26], thus obtaining a larger R_s value (≈24%) compared to the result derived from Eq. (5).

Dry deposition will take place only as a result of removal from the air to the surface. Such being the case, surface properties, as reflected by R_c, are very important in the final stage of the dry deposition process for gases. Zhang et al. [30] presented a model for R_c, which, in essence could be described by:

$$\frac{1}{R_c} = \frac{1 - W_{st}}{R_{st} + R_m} + \frac{1}{R_{ns}} \quad (6)$$

where

$$\frac{1}{R_{ns}} = \frac{1}{R_{cut}} + \frac{1}{R_{ac} + R_g} \quad (7)$$

The variable W_{st} is the fraction of stomatal[1] blocking under wet conditions. R_{st} is the stomatal resistance calculated using a sunlit/shade stomatal resistance submodel [32] and R_m is the mesophyll[2] resistance dependent only on the chemical species [32]. R_{ns} is the non-stomatal resistance, which further is broken down into resistance to the cuticle[3] uptake, R_{cut}, and resistance to the soil uptake including in-canopy aerodynamic resistance, R_{ac}, and the soil resistance, R_g. The variables R_{st}, R_m, R_{ac}, and R_{cut} are not applicable for land without canopies. To use Eqs. (6) and (7) for such land, R_{ac} is set to 0 and R_{st}, R_m, and R_{cut} to a very large value, i.e. $R_c = R_{ns} = R_g$. Numerical values for R_g are suggested [30].

The non-stomatal resistance, R_{ns}, parameterizes for SO_2 and O_3 as a function of friction velocity, relative humidity, leaf-area index (LAI), and canopy wetness [30]. Non-stomatal resistance for other chemical species can be scaled to those of SO_2 and O_3 based on their characteristics, such as solubility and half-redox reactivity [33]. It is worth noting that in the model by Zhang et al. [30], the canopy cuticle resistance is separately calculated for dry and wet conditions and that both the soil resistance and the resistance to the cuticle uptake are adjusted according to a snow-cover fraction.

Fig. 1 illustrates the variation due to wind speed (Fig. 1a) and stratification (Fig. 1b) of the sub-layer resistance for SO_2, R_s, and the aerodynamic resistance, R_a, in the atmospheric surface layer calculated for a cloud thickness determined at a distance of 10 km. In Fig. 1a it can be seen that both R_s and R_a decrease when the wind speed increases. Fig. 1b shows that R_s increases somewhat while R_a decreases for more stable conditions. Based on the model by Zhang et al. [30], the highest value of v_d for SO_2 (7.5 cm/s) presented by Sehmel [1] (see Section 1) seems to be very rare.

3. Dispersion models

Many advanced dispersion models like VLSTRACK [34], HPAC/SCIPUFF [35], ADPIC [36–39] and MATCH [40] allow for three-dimensional time-dependent meteorological input provided by mesoscale models. For example, HPAC/SCIPUFF may require both three-dimensional meteorological mean fields (e.g. wind and temperature) and two-dimensional boundary conditions (e.g. friction velocity, surface roughness, and sensible heat flux.) While this high functionality may increase the accuracy and capability of real applications, it is thought to be of less benefit in illustrating the influence of dry deposition on dispersion since simpler wind fields, terrain descriptions, etc., make the results more clear. Therefore, two simple analytical models and one somewhat more complex Lagrangian model with Langevin formulation (LEM model) were used for the simulations. The LEM model utilized only horizontally homogenous wind fields.

3.1. Box-type models

Two box-type models were used since dry deposition can be explicitly formulated in such models. The effects of dry deposition are therefore easier to understand, identify and discuss.

3.1.1. Continuous source model

Following the work of Scriven and Fisher [41], a two-dimensional dispersion in the x–z plane is considered, where x is a horizontal coordinate and z a vertical coordinate. If $C(x)$ is the concentration at distance x, the rate at which the contaminant crosses a vertical plane is $u(x)H(x)L(x)C(x)$, where u is the horizontal velocity perpendicular to the plane, H is the height of the plane, L is the lateral extension of the plane and C is the concentration at the plane. Eq. (1) defines the deposition velocity [24], v_d. Neglecting any other loss except loss to the bottom and assuming $u(x)$ = constant, the mass-balance equation for $C(x)$ is:

$$u\frac{d}{dx}(H(x)L(x)C(x)) = -v_d L(x)C(x) \quad (8)$$

If

$$L(x) = L_0 + 2\theta_y x \quad (9)$$

where L_0 is the lateral extension at the source and θ_y is the lateral dispersion parameter, then Eq. (8) has a well-known solution if θ_y and H do not depend on x (Eq. (10)) [34],

[1] Small pores in the outer layer of a leaf or stem through which gases and water vapor pass. Also called stomata.
[2] The photosynthetic tissue of a leaf.
[3] A covering layer of wax-like, water-repellent material.

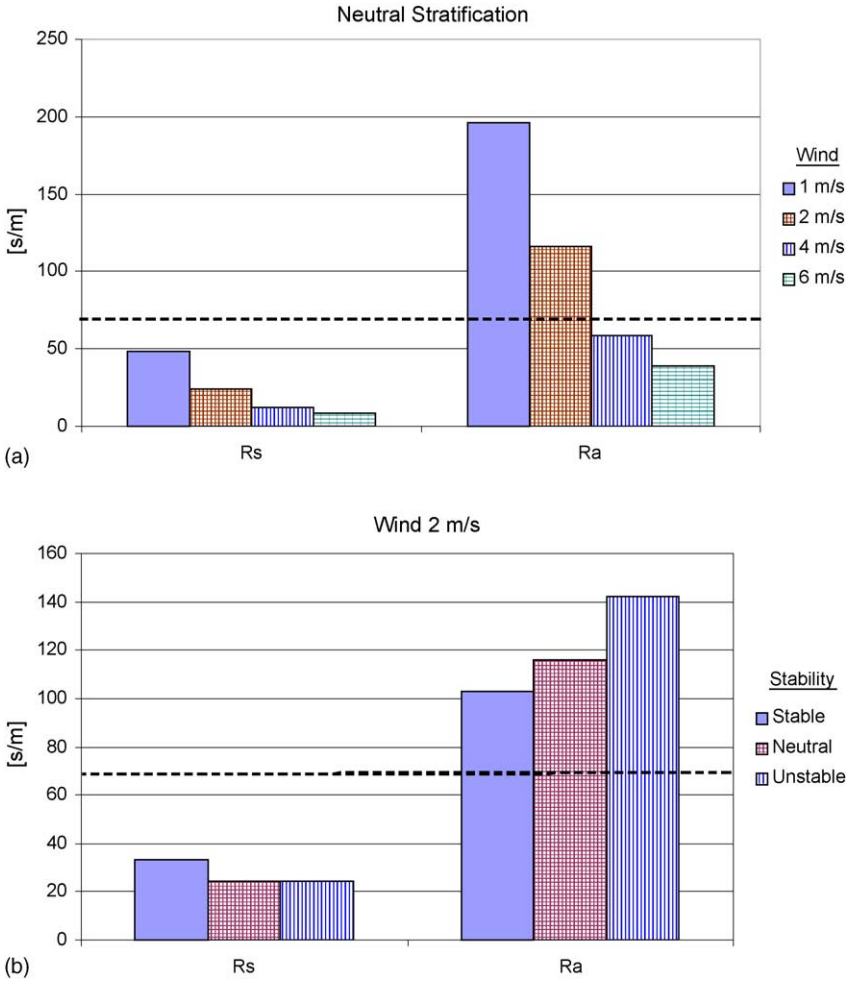

Fig. 1. (a) Variations by wind speed of the sub-layer resistance for SO_2, R_s, and the aerodynamic resistance, R_a, in the atmospheric surface layer calculated for a cloud thickness determined at a distance of 10 km in the case of neutral stratification; (b) illustrates how R_s, and R_a are affected by different stratification cases (Pasquille types C, D and E determined, according to [17], c.f. Table 1) for a cloud thickness determined at a distance of 10 km for a wind speed of 2 m/s. The dashed lines represent the surface (canopy) resistance for SO_2, R_c, during wet days.

which describes the variation in concentration in the downwind direction of a continuous source under perfect mixing conditions. Thus, if $H = H_m$ is thought of as the height of the mixing layer and ϕ_y = the constant value of θ_y, then

$$C(x) = C_0 \frac{1}{(1 + 2\phi_y(x/L_0))} e^{-(v_d/H_m)x/u} \quad (10)$$

(the different variables defined above). Scriven and Fisher use a ϕ_y value of 0.08 for long-range dispersion. To study the long-range transport of pollutants [18,34], several researchers have used Eq. (10), though there are many approaches that can be taken [42,43]. However, in this study the distance-dependent lateral dispersion parameters for conditions pertaining to open country recommended by Briggs [44] for different Pasquille-type stability classes were used [45,46].

3.1.2. Puff model

To derive an analytical model equation for a simple three-dimensional homogenous puff including dry deposition where the puff is located at ground level, one approach could be to extend Eq. (10) by a simple mass-balance consideration for a puff, yielding:

$$C(x) = C_0 \frac{1}{(1 + 2\Phi_y(x/L_0))} \frac{1}{(1 + 2\Phi_x(x/S_0))} \times \frac{1}{(1 + ((\Phi_z x)/H_0))} e^{-(v_d/H_0 + (\Phi_z x))^{x/u}} \quad (11)$$

where C_0 is the initial concentration in the source volume defined by $L_0\ S_0 H_0$, L_0 is the source extent in the cross-wind direction, S_0 the source extent in the wind direction and H_0 the height of the source. The distance-dependent lateral and vertical dispersion parameters for open country conditions recommended by Briggs [44] for different Pasquille-type stability classes [45,46] are denoted by Φ_x, Φ_y, and Φ_z. The variable x is the distance from the source location and u is the (constant) wind speed. An explanation of the reasoning behind the variation of H in the downwind direction can be found in the Appendix. As the dispersion

parameters depend on the distance to the source, x, Eq. (11), as well as Eq. (10), do not strictly represent correct solutions. However, these equations can be expected to render good approximations, as is illustrated in the Appendix for Eq. (11).

These two types of box-like models (Eqs. (10) and (11)) were used in this study with the modification that the height of the clouds is restricted to the mixing-layer height. From Eqs. (10) and (11) it can be seen that the dry deposition effect is approximately expressed by $e^{-v_d x/Hu}$, where H is now a mean vertical extent of the cloud. A low H value, that is stable stratification, and a low wind velocity, u, lead to a greater dry-deposition effect. For example, a ground release of $H = 30$ m, $u = 1$ m s^{-1}, $v_d = 0.01$ m s^{-1} and $x = 3000$ m results in $e^{-v_d x/Hu} \approx e^{-1} \approx 0.37$, which shows that the concentration is reduced by 63% after 3000 m. However, v_d also needs to be formulated according to H and u (see Eqs. (3)–(7)). In these equations the micrometeorological variables are determined from the Monin-Obukhov similarity profile relations [28]. Furthermore, in the box models the wind speed u is independent of height. Hence, all the different parameters in Eqs. (3)–(7) can be given specific and constant values for each case studied.

3.2. Langevin formulation of lagrange model

One drawback of the box-type models is that the concentration is constant with height, which might lead to an underestimation of the deposition flux, especially for a source located at ground level. Another drawback is the constant wind-height profile (both speed and direction). Therefore, a Lagrange approach to turbulent dispersion was also employed in the investigation. The Lagrange approach originates from Taylor's classic (1921) paper 'Diffusion by Continuous Movements' [47]. Taylor argued that the transport of species due to molecular diffusion is negligible compared to advective and turbulent transport and consequently the mean flow field can be evaluated from data on the motion of fluid particles. Compared to the box-type models, a more realistic concentration and wind profile is implemented in the Lagrange model used. Variations in height in both the wind and turbulence fields are considered. Taylor argued, regarding the model, that the dispersion of a passive substance is computed by tracing the motion of fictive particles, which can represent air parcels or aerosol particles. These fictive particles are assumed to represent the ensemble average values of the actual particle distribution. By allotting a certain amount of the substance to each particle, the coupling to the total amount of substance is represented. Small and light particles follow turbulent fluid fluctuations so their particulate diffusivity is identical to the fluid eddy diffusivity [48]. Thus, it should be possible to follow the turbulent motion in eddies by supplementing the Lagrange approach with a sufficient model of the velocity of a fluid particle in turbulence such as the Langevin model (LEM) [49] (originally proposed by Langevin (1908) [50]). The Lagrange model used in this investigation [51,52] is based on the Langevin equation.

The Langevin equation can be formulated as:

$$\frac{\mathrm{d}x(t)}{\mathrm{d}t} = Ax(t) + \xi(t) \tag{12}$$

where $x(t)$ is a $p \times 1$ random vector representing position. The variable p is the number of particles in the model, A is a $p \times p$ matrix, $\xi(t)$ is a $p \times 1$ random vector whose correlation matrix satisfies

$$R_\xi(t, \tau) = \left\langle \xi(t+\tau)\xi^*(t) \right\rangle \rightarrow R_\xi(\tau) \tag{13}$$

where ξ^* stands for conjugated transposed.

The application of similar stochastic differential equations to turbulent diffusion began several decades ago and includes homogenous turbulence [53] as well as inhomogeneous turbulence [54] and skewed turbulence [55]. In the specific LEM model used in our study the boundary-layer height and wind profile is modelled, ccording to Zilitinkevich et al. [56]. Implementation of the Langevin equation for stable and neutral stratification is achieved as follows:

$$\begin{cases} \mathrm{d}x_i = u_i \mathrm{d}t \\ u_i = u_{i,\mathrm{old}} + \mathrm{d}u_i \\ \mathrm{d}u_i = a_i(\vec{x}, \vec{u}, t)\mathrm{d}t + b_{i,j}(e)\mathrm{d}W_j(t) \end{cases} \tag{14}$$

where $\mathrm{d}W_j(t)$ represents an increment in a Wiener process with an expected mean of 0 and deviation $\mathrm{d}t$. The functions a_i and $b_{i,j}$ are a deterministic and stochastic acceleration, respectively. For unstable stratification, the correlation between the lateral and vertical velocity components is neglected. This model uses the dry deposition velocity to calculate the probability that model particles reach and are deposited on the surface [21]. This deposition probability is expressed by:

$$P = \frac{\phi_\mathrm{m}}{\phi_\mathrm{p}} = (2\pi)^{1/2}\frac{v_\mathrm{d}}{\sigma_\mathrm{w}} \tag{15}$$

where ϕ_m is the mass flux through any given surface, ϕ_p is the mass flux in the negative z direction through a surface in the case of a Gaussian velocity distribution with a zero average velocity and a standard deviation σ_w [57]. The use of a deposition probability entails that there is no need for a local value of concentration in the dry-deposition calculation. This deposition algorithm was verified against carefully controlled deposition experiments by Karlsson et al. [21]. Furthermore, since the overall deposition in the Lagrange model is applied very close to the surface and the turbulent transfer calculation is inherent in the model, the aerodynamic resistance becomes insignificant, i.e., it would have a value close to zero. Similar approaches were already reported by Boughton [58] and Wilson [59] and are nowadays quite common. In the model used in this investigation, the dry-deposition rate can be given as a fixed-value data input, or, alternatively, it can be calculated according to a model presented by Zhang et al. [60]. No special heavy-gas effects are taken into account in either of the box models or the LEM model. However, a pancake-like

source is used in one case to partly simulate the effects of dry deposition on heavy-gas clouds.

4. Results

The main question we wanted to answer with this investigation was whether or not, due to dry deposition, the concentration from a ground release of hazardous gas would be lower in stable stratification than in neutral or unstable stratification, and if so, under which particular conditions. We also wanted to quantify how the effect of dry deposition is influenced by release height for some conditions. For this purpose, we used the three different models presented in Section 3 to simulate the effect in a number of cases divided into three scenarios: an instantaneous ground-level release, an instantaneous elevated release and a continuous release. The simulations were often extended to 100 km where dispersion models are not usually verified by experiments. Therefore, we do not expect the absolute concentration levels to be highly reliable. However, since this study focused on the relative effect of dry deposition rather than its absolute consequences and, furthermore, used a well-established formulation for the dry deposition process, it is believed that the effect of this uncertainty is not detrimental to the purpose of this study.

In this section the results of the investigation are presented. In the next section, Section 5, the findings from the simulations of each of the scenarios are summarized and discussed. One neutral and one stable weather case is defined for each of the scenarios used in this investigation. Also, one unstable case is defined in two of the scenarios. The specific data used for each weather condition can be found in Table 1. Other specific data common to all scenarios are the kinematic viscosity of air ($v_d = 1.6 \times 10^{-5}\ m^2\ s^{-1}$), the molecular diffusivity of the substance in air ($D_{sarin} = 6.9 \times 10^{-6}\ m^2\ s^{-1}$ [61], $D_{VX} = 4.8 \times 10^{-6}\ m^2\ s^{-1}$ [61], $D_{SO2} = 1.3 \times 10^{-5}\ m^2\ s^{-1}$), roughness height ($z_0 = 0.3$ m), Coriolis parameter (1.15×10^{-4}) and the von Karman constant ($\kappa = 0.41$).

4.1. Instantaneous release

This puff-type release was investigated using both an analytical puff model, Eq. (11), and the more sophisticated Lagrange LEM model described in the preceding section. The extension of the source was set to 10 m × 10 m × 10 m (in one case 31.6 m × 31.6 m × 1 m) and the initial concentration arbitrarily to 10^5 mg/m^3.

As a starting point, the Lagrange LEM model was used to identify the expected situation for a zero dry deposition velocity. This is illustrated in Fig. 2a (ground release) and 2b (elevated release), where the calculated maximum ground-level concentration versus distance from a 10 m× 10 m × 10 m instantaneous release with a wind speed of 2 m s^{-1} is presented. Also, in order to understand how the LEM model results and the box-type puff model results would relate, it was deemed of value to compare dispersion as predicted by each model without dry deposition (i.e. $v_d = 0$) for a stable and a neutral weather situation. This is also shown in Fig. 2a where it can be observed that the two model types rendered quite similar predictions for neutral stratification while the box-type puff model predicted less dispersion for stable stratification. It can also be seen in Fig. 2, and in all the following curves representing results from the LEM model, that the curves are not perfectly smooth. This is mainly due to some randomness built into the model that results in several maximum values in the cloud appearing as the cloud grows, thus making the exact determination of the location of the maximum point difficult. To deal with this problem, a statistical procedure was adopted but in spite of this effort some randomness can still be found in curves plotted from the LEM model results.

4.1.1. Ground-level release

How dry deposition affects the calculated maximum concentration for an instantaneous ground-level release is first illustrated in Fig. 3 by using the box-type puff model where the dry deposition velocity was calculated for sarin, SO_2 and VX for stable, neutral and unstable stratification. It can be seen in Fig. 3 that the influence of dry deposition lowers the concentration more in the case of stable stratification than in the case of neutral or unstable stratification. Heuristically, given the initial amount in the release, the low mixing layer in stable stratification favors dry deposition at an early stage because the smaller mixing volume means a higher concentration, and thereby a higher dry-deposition rate. If the gas cloud does not move too fast and the deposition rate is high

Table 1
Specific data used for each weather condition

Stability	Wind (10 m) [m s^{-1}]	The height of the boundary layer [m]	Monin-Obukhov length [m]	Friction velocity [m s^{-1}]	Stability
Stable	1	49	50	0.085	E
Neutral	1	176	10^9	0.115	D
Unstable	1	1500	−9	0.138	A
Stable	2	69	50	0.168	E
Neutral	2	347	10^9	0.23	D
Unstable	2	1500	−50	0.23	C
Stable	4	89	50	0.32	E
Neutral	4	680	10^9	0.457	D
Unstable	4	1500	−50	0.46	C

Stability determined in accordance with the work of Hanna et al. [17].

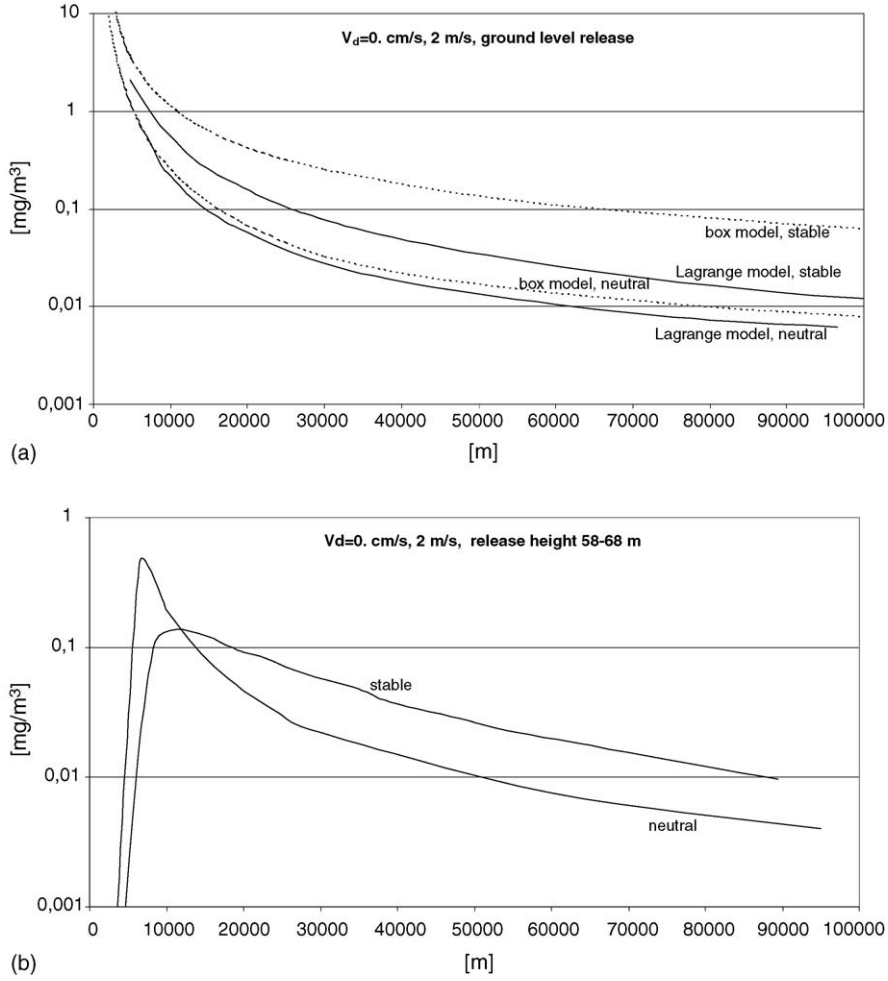

Fig. 2. The figure illustrates the situation without dry deposition and shows the calculated maximum ground-level concentration vs. distance from a 10 m × 10 m × 10 m instantaneous release where the wind speed is 2 m s^{-1}. The maximum concentration is calculated for stable and neutral stratification using a Lagrange LEM model: (a) shows the situation for a ground-level release while (b) shows the situation for a release extending from a height of 58–68 m. Also, (a) shows the difference between the predictions of dispersion without dry deposition ($v_d = 0$) as predicted by the two model types used, a Lagrange LEM model and a box-type puff long range model, respectively, for both a stable and a neutral weather situation.

enough, a condition will eventually arise; the gas concentration in the low mixing layer will be reduced to the same level as the one in the higher mixing layer present in neutral stratification. From that point in time, when the concentrations, and thus the deposition rates, are equal, the concentration in the low mixing layer will decrease faster as the cloud moves because of the smaller volume of gas (mass) represented by the lower mixing layer. The difference in deposition velocity among VX, SO_2 and sarin for a wind speed of 2 m s^{-1} does not seem to affect the concentration much during unstable stratification and, only marginally, during neutral. However, a clear difference can be seen for stable stratification among sarin, SO_2 and VX. For VX, the concentration for a stable stratification is lower than for a neutral stratification after about 70 km and lower than for an unstable stratification after more than 100 km. In Tables 2 and 3, the corresponding intersections of concentration curves for stable-neutral and stable-unstable stratification, with wind speeds of 1 m s^{-1} and 4 m s^{-1}, can also be found. The intersection of the con-

Table 2
Intersecting of stable and neutral curves for different substances for a ground release of 10 m × 10 m × 10 m

Wind [m s^{-1}]	Distance from source [km]		
	Sarin	VX	SO_2
1	60	49	50
2	107	72	87
4	>100	104	>100

Figures from analysis using a box-type puff long-range model equation.

Table 3
Intersecting of stable and unstable curves for different substances for a ground release of 10 m × 10 m × 10 m

Wind [m s^{-1}]	Distance from source [km]		
	Sarin	VX	SO_2
1	106	86	88
2	>100	>100	>100
4	>100	>100	>100

Figures from analysis using a box-type puff long-range model equation.

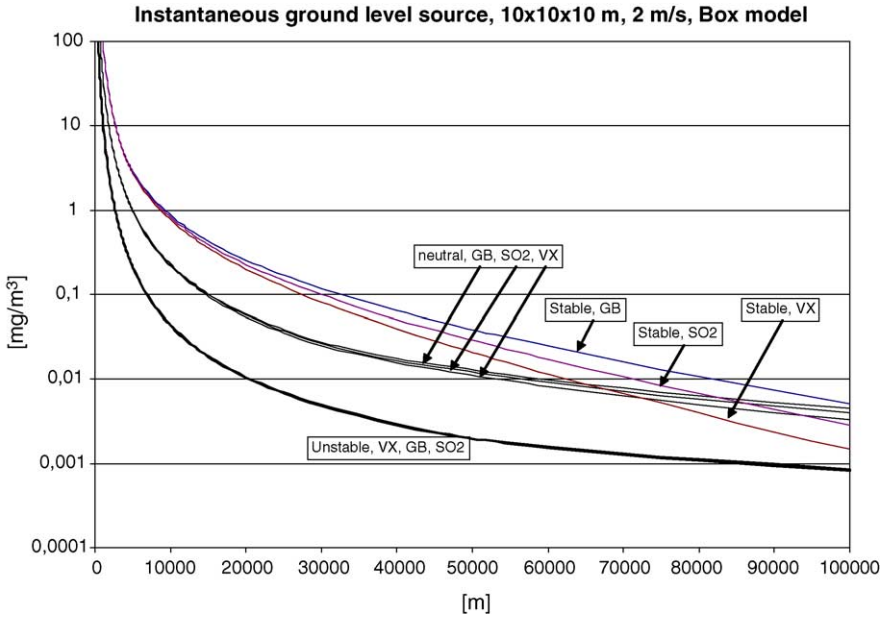

Fig. 3. The figure illustrates the effect of dry deposition for different micrometeorological conditions using a box-type long-range puff model and shows the calculated maximum concentration for a wind speed of 2 m s^{-1} vs. distance from a 10 m × 10 m × 10 m instantaneous release at ground level. The concentration is calculated for stable, neutral and unstable stratification. Different curves are shown where dry deposition resistance is calculated for sarin, SO_2 and VX, respectively.

centration curves is contrary to what was found without dry deposition (Fig. 2a).

The fact that the comparisons are made between two stabilities, both having the same wind speed, should not be a serious restriction since, as illustrated in Fig. 3, dry deposition mainly has an effect in stable stratification. For example, in the case of VX, the distance to the intersection of the curve representing stable stratification with a wind speed of 1 ms^{-1} and the curve representing neutral stratification with a wind speed of 6 ms^{-1} is 52 km. This is an increase of only about 6% compared to the corresponding distance when both wind speeds are 1 ms^{-1}, i.e. the distance to the intersection increases from 49 km (Table 2) to 52 km.

For comparison, the calculated maximum concentration using a Lagrange LEM model is shown in Fig. 4 for stable and neutral stratification with a wind speed of 2 m s^{-1} and a dry deposition velocity matching VX. With a source extending from the ground to a height of 10 m (hereafter referred to as release height 0–10 m) it can be seen in Fig. 4a that the concentration for a stable stratification becomes lower than for neutral stratification after around 32 km, contrary to what was observed with no dry deposition, i.e. $v_d = 0$ (Fig. 2a). Illustrating the results for a release height of 0–1 m, Fig. 4b shows that the concentration for a stable stratification becomes lower than for neutral stratification after approximately 14 km, which is less than half the distance for the higher source height (Fig. 4a).

4.1.2. Release at 58–68 m

This puff-type release was investigated using only the Lagrange LEM model. As for the ground release, the extension of the source was set to 10 m × 10 m × 10 m and the initial concentration arbitrarily to 10^5 mg/m^3, but instead of being located at ground level, in this scenario the source was located 58 m above the ground, i.e. just beneath the boundary-layer height for the 2 m s^{-1} stable stratification.

In Fig. 5, the calculated maximum concentration at ground level versus horizontal distance from the instantaneous elevated release is shown. The wind speed is 2 m s^{-1} and the dry deposition velocity resembles the value for VX, i.e. 1.4 cm s^{-1} for stable stratification and 1.8 cm s^{-1} for neutral stratification. It can be observed that the calculated maximum concentration at ground level for stable stratification reaches its highest value further away from the source than does the concentration for neutral stratification. Once the concentration for stable stratification becomes higher than for neutral stratification, it does not decrease below the corresponding curve for neutral stratification for distances shorter than 100 km, which is in line with the case without deposition (Fig. 2b).

4.1.3. Differences in the influence of dry deposition on a ground-level and elevated release

As a comparison, Fig. 6 shows the calculated maximum concentration at ground level versus horizontal distance from an instantaneous 10 m × 10 m × 10 m elevated release (58–68 m above ground level, dotted curve) and a ground-level release (solid curve). In Fig. 6a, both ground and elevated releases are shown for neutral stratification and a v_d of 1.4 cm s^{-1}. In Fig. 6b, both ground and elevated releases are shown for stable stratification and a v_d of 1.4 cm s^{-1}. All curves in the figure represent a wind speed of 2 m s^{-1}. The

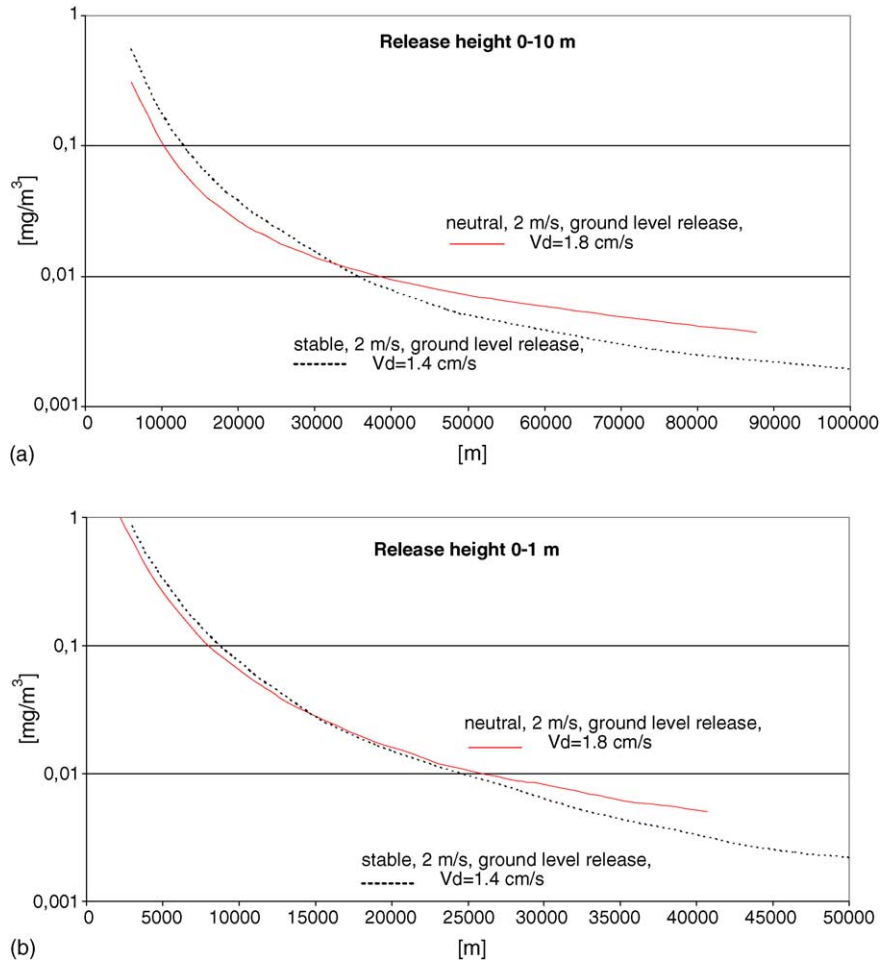

Fig. 4. The figure illustrates the effect of dry deposition in different micrometeorological conditions using a Lagrange LEM model and shows the calculated maximum concentration vs. distance from an instantaneous release at ground level for a wind speed of $2\,m\,s^{-1}$ and a dry deposition velocity matching VX. The maximum concentration is calculated for stable and neutral stratification; (a) shows the situation for a $10\,m \times 10\,m \times 10\,m$ release, (b) shows the situation for a source with height 1 m and a volume equal to the source in (a). Note the different scales on the *x*-axis in (a) and (b).

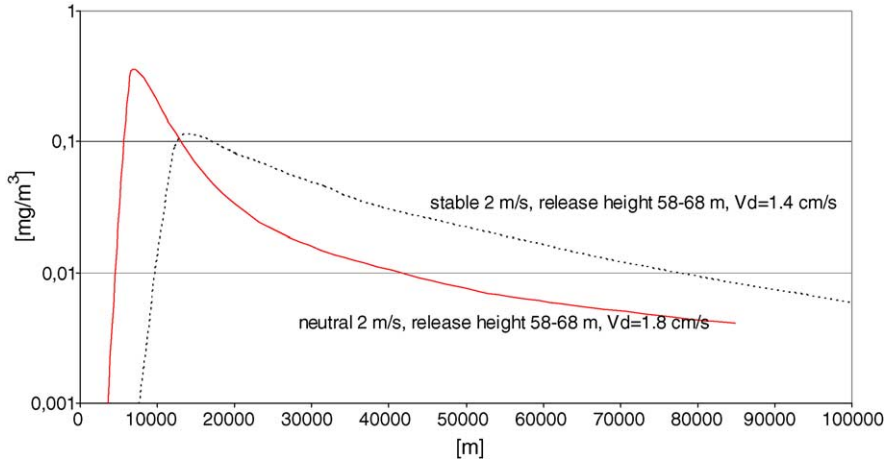

Fig. 5. The figure shows calculated maximum concentration at ground level vs. horizontal distance from a $10\,m \times 10\,m \times 10\,m$ instantaneous high-source-height release (58–68 m above ground level) for a wind speed of $2\,m\,s^{-1}$ and a dry deposition velocity matching VX. The maximum concentration is calculated for stable and neutral stratification using a Lagrange LEM model.

figure reveals that for both stable and neutral stratification, the concentration at ground level for the elevated release reaches its maximum value shortly after it exceeds the corresponding concentration for the ground-level release. Moreover, once the concentration for the elevated release becomes greater than that for the ground-level release, it does not decrease below the curve for the ground-level release, although the difference between the two neutral-stratification cases in Fig. 6a

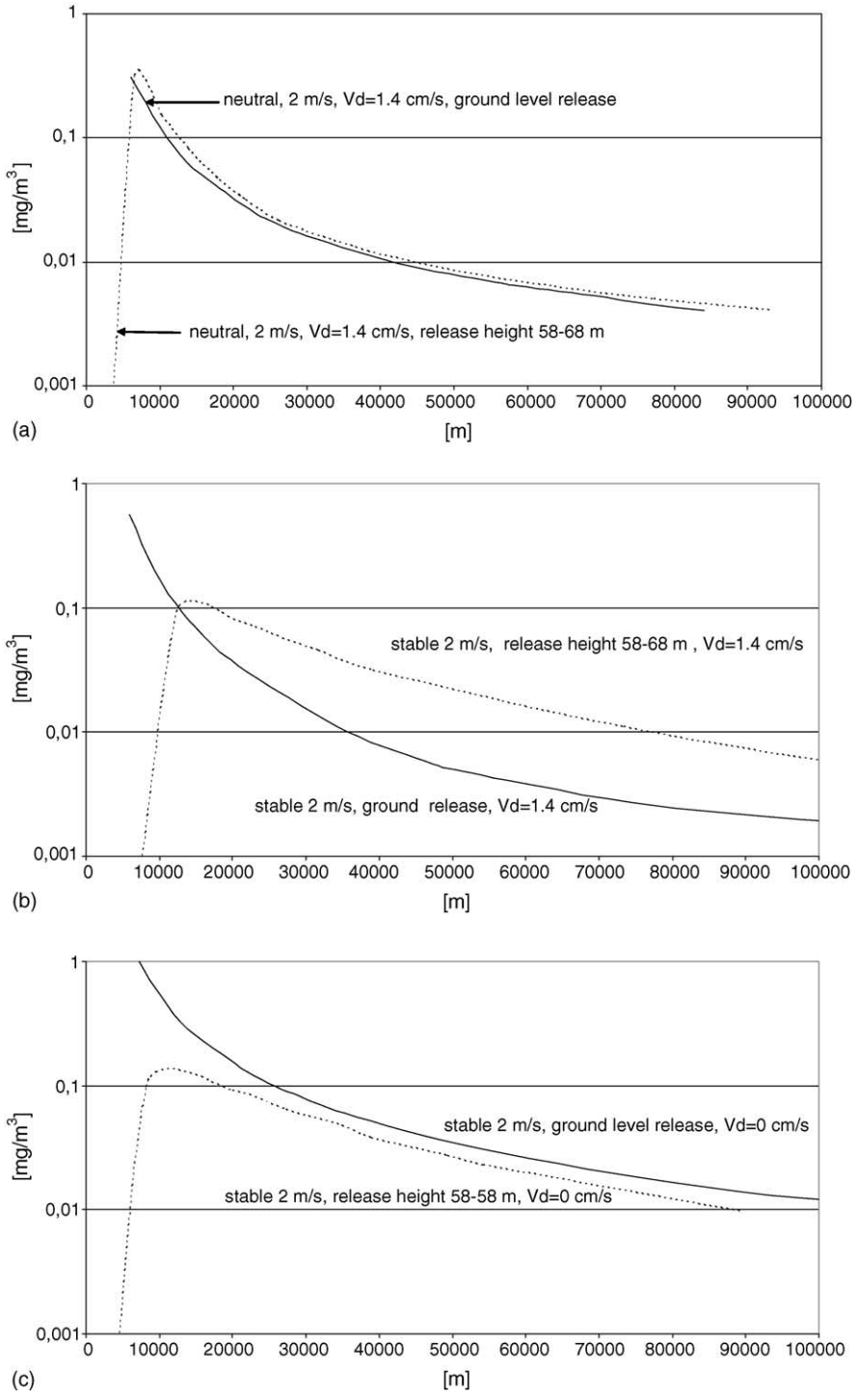

Fig. 6. Calculated maximum concentration at ground level vs. horizontal distance from a 10 m × 10 m × 10 m instantaneous high-source-height release (58–68 m above ground level, dotted curve) and a ground-level release (solid curve). In (a) high and low heights of the sources are compared for neutral stratification and a v_d of 1.4 cm s^{-1}. In (b) high and low heights of the sources are compared for stable stratification and a v_d of 1.4 cm s^{-1}. All cases represent a wind speed of 2 m s^{-1}. The maximum concentration is calculated using a Lagrange LEM model. Once the concentration for the high release becomes greater than that for the ground-level release, it does not decrease below the curve for the ground-level release. This is opposite the situation with no dry deposition ($v_d = 0$) where the ground release renders a higher concentration for all distances (c).

Table 4
Approximate time in seconds up to the point where half of the total amount from a ground release of 10 m × 10 m × 10 m has deposited

Stability	Approximate time [s] until total airborne amount is reduced by 50% due to dry deposition only (wind 2 ms^{-1})					
	Ground level release (0–10 m)				High release (58–68 m)	
	v_d = 0.8 [cm s^{-1}]	v_d = 1.1 [cm s^{-1}]	v_d = 1.4 [cm s^{-1}]	v_d = 1.8 [cm s^{-1}]	v_d = 1.1 [cm s^{-1}]	v_d = 1.4 [cm s^{-1}]
E	3000	2400	1790	1320	14,000	13,200
D	18,000	13,200	9600	7200	21,600	19,200

The figures in the table are from calculations using the Lagrange LEM model.

is very small after approximately 25 km. This is opposite to what was found for the situation with no dry deposition (v_d = 0) where the ground release rendered a higher ground-level concentration for all distances (Fig. 6c).

4.1.4. Half-value time and half-value distance

The time up to the point where half of the initially airborne amount has deposited, as calculated (LEM simulation) for both a ground release and an elevated release, can be found in Table 4. Obviously, this half-value time decreases with an increasing deposition velocity for both types of releases. Also, the half-value time due to dry deposition is considerably larger for the elevated release than for the ground level. Furthermore, this difference between ground-level and elevated releases seems to be somewhat increasing with an increasing deposition velocity. In the case of a ground-level release, the half-value time for the neutral case (stability D) is 5.4–6 times larger than the corresponding time for the stable case (stability E) while the corresponding relation is approximately 1.5 for the elevated release. Interestingly, the half-value time also seems to be roughly inversely proportional to the dry deposition velocities within stability class and release type.

The approximate distances until the total airborne amount is reduced by 50% due to dry deposition could also be heuristically compared to the data presented by Hanna et al. [17], i.e. half-value distances for source heights of 0, 10 and 50 m, a wind speed of 1 m s^{-1} and dry deposition velocity of 1.0 cm s^{-1}. The comparison is illustrated in Table 5. It is worth noting that the zero-height data presented by Hanna et al. are greater than those calculated in this study representing the ground-level release (0 m). However, this study's calculations resulted in larger half-value distances for all other cases.

In order to obtain a better understanding of how sensitive the data in Table 5 is to changes in assumptions reflected in input data, Table 6 shows the calculated half-value distances compared to corresponding data for a wind speed of 2 m s^{-1} instead of 1 m s^{-1} and more diffuse sources, i.e. with source extensions of 10 × 10 × 10 m like those used in other calculations in this investigation instead of 1 m × 1 m × 0.01 m as used in the comparison with data presented by Hanna et al. As expected, the combined effect of the doubling of the wind speed and a more diffuse source was found to be significant, resulting in at least a doubling of the half-value distance in most cases. One exception was the stable stratification case where the source was elevated/extended to 10 m above the ground. For the lower wind-speed case (1 m s^{-1}), the fact that all the physical extension of the source was elevated tended to increase the half-value distance, while at the same time the lower wind speed tended to decrease it. Regarding the corresponding neutral case, the higher turbulence and mixing layer made this case much less sensitive to the elevation of the source.

The data presented for the zero-height release case in Tables 5 and 6 can be used to estimate the effect of dry deposition on the evaporating vapor from a pool of a liquid chemical, e.g. Cl_2, NH_3, or HF, for which v_d can be estimated to be about 1–2 cm s^{-1} at a wind velocity equal to 1–2 m s^{-1}.

Table 5
Heuristic comparison of some values presented by Hanna et al. and Lagrange LEM calculations of distances in kilometers at which 50% of the released amount is depleted by dry deposition for stability classes D and E

Stability	Approximate distance [km] until total airborne amount is reduced by 50% due to dry deposition only					
	Low height release				Higher height release	
	Hanna et. al. [17]		Present (LEM) calculation		Hanna et. al. [17]	Present (LEM) calculation
	v_d = 1.0 [cm s^{-1}] Wind 1 [m s^{-1}] Height		v_d = 1.0 [cm s^{-1}] Wind 1 [m s^{-1}] Height		v_d = 1.0 [cm s^{-1}] Wind 1 [m s^{-1}] Height	v_d = 1.0 [cm s^{-1}] Wind 1 [m s^{-1}] Height
	0 [m]	10 [m]	0 [m]	10 [m]	50 [m]	49 [m]
C	1.8	18			43	
D	0.4	3.5	0.2 (0.3)	14 (18)	8.6	26 (32)
E	0.15	2.2	0.04 (0.1)	4.2 (6.5)	8.3	30 (35)

The present calculation figures represent the distance between the source and the maximum concentration in a 10-m high layer above the ground. The figures within parentheses represent the approximate distance to the front of the cloud in the same layer. The extension of the sources in the LEM simulation is 1 m × 1 m × 0.01 m.

Table 6
Illustration of sensitivity to changes in input data shown by a comparison of values of distance in kilometers at which 50% of the released amount is depleted by dry deposition for wind speeds of 1 and 2 m s^{-1} and different source extensions

Stability	Illustration of sensitivity to changes in input data showing the effect of wind and diffuse source extent on approximate distance [km] until total airborne amount is reduced by 50% due to dry deposition only					
	Low height release				Higher height release	
	Wind 1 [m s^{-1}]		Wind 2 [m s^{-1}]		Wind 1 [m s^{-1}]	Wind 2 [m s^{-1}]
	v_d = 1.0 [cm s^{-1}] Height		v_d = 1.1 [cm s^{-1}] Height		v_d = 1.0 [cm s^{-1}] Height	v_d = 1.1 [cm s^{-1}] Height
	0 [m]	10 [m]	0–1[m]	0–10 [m]	50 [m]	58–68 [m]
D	0.2 (0.3)	14.4 (18)	12 (15)	42[a] (51)	26 (32)	67 (83)
E	0.04 (0.1)	4.2 (6.5)	1 (1.7)	5.7[b] (12)	30 (35)	77 (86)

The figures represent the distance between the source and the maximum concentration in a 10-m high layer above the ground. The figures within parentheses represent the approximate distance to the front of the cloud in the same layer.
[a] The corresponding value for the box-type model (Eq. (11)) is 22 km.
[b] The corresponding value for the box-type model (Eq. (11)) is 4.4 km.

The half-value distance at neutral and stable stratification is <500 m, indicating a strong reduction in the gas concentration. The 0–1 m source-height data in Table 6 can be used to estimate the effect of dry deposition on a pancake-like cloud of a heavy gas released from a ruptured tank containing, e.g. Cl_2, NH_3. The half-value distance is 1 km for 2 m s^{-1} at stable stratification, which indicates a strong effect. These two examples show the need to consider dry deposition in risk-analysis dispersion models for industrial chemicals.

4.2. Continuous release

This type of release was investigated using only an analytical model, Eq. (10). The extension of the source was set to $H \times 500$ m and the initial concentration, C_0, arbitrarily to 10^2 mg/m^3 for unstable weather conditions with a wind speed of 2 m s^{-1} for which the height of the boundary layer, H, is 1500 m (Table 1). Under other weather conditions, C_0 is scaled by Hu, where u is the wind speed, to preserve the rate of totally released amount per second among the micrometeorological cases.

In Fig. 7, where the calculated dry deposition velocity is presented for VX in all cases (wind velocity of 2 m s^{-1}), it can be observed that the concentration for stable stratification becomes lower than for neutral stratification after about 53 km and lower than for unstable stratification after about 85 km. This differs from the situation with no dry deposition (v_d = 0), where no intersecting of the curves would occur and stable stratification would give the highest concentration for all distances. It also differs from the scenario of an instantaneous release in that the distance to the intersection points is shorter, although the influence of the dry deposition velocity manifests itself in the same way.

In Table 7, the corresponding intersections of concentration curves for stable/neutral and stable/unstable stratification for wind speeds of 1 and 4 m s^{-1} can be found. For example, the concentration for stable stratification becomes lower than that for neutral stratification after about 32 km and low-

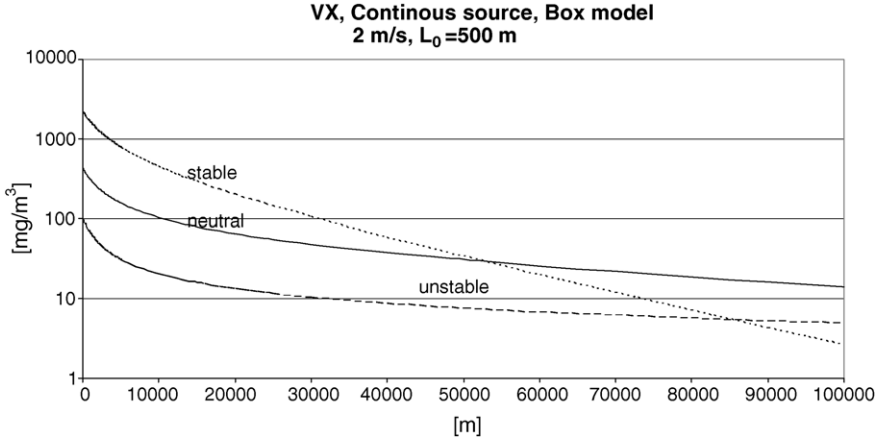

Fig. 7. Calculated concentration for stable, neutral and unstable stratification using a box-type long-range model for a 500-m wide continuous release with the height given by the boundary layer. The dry deposition velocity is calculated for VX. The figure shows the situation for a wind speed of 2 m s^{-1}.

Table 7
Intersecting of stable and neutral curves and stable and unstable curves, respectively, for the substance VX for a ground release $H \times 500$ m

Wind [m s^{-1}]	Distance from source [km] VX	
	Stable/neutral intersection	Stable/unstable intersection
1	32	60
2	53	85
4	83	112

Figures from calculations using a box-type continuous-source long-range model.

ers than for unstable stratification after about 60 km with a wind speed of 1 m s^{-1}.

5. Summary and discussion

Despite the fact that dry deposition nowadays is a common process implemented in atmospheric dispersion models, few studies have been carried out on its effect on the concentration of hazardous gases for different atmospheric stratifications and release heights. This investigation focused on how dry deposition influences the concentration of toxic gas clouds. We specifically investigated the conditions under which it could be expected that neutral or even unstable stratification might render higher concentrations than stable stratification due to the effect of dry deposition when proper consideration is given to the variation in different parameters governing the dry deposition velocity. The influence on the reliability of the investigation findings of any serious drawback associated with one of the particular models used is counteracted by the utilization of different model types which are thought to complement each other in different ways, and also by the selection of release cases.

5.1. Dry deposition velocity

Data on dry deposition velocity for hazardous gases is scarce. Only a few data points on values up to some cm s^{-1} are available. Since many toxic gases are highly reactive and/or water miscible, the surface (canopy) resistance, r_c, is expected to be low for vegetated surfaces. In that case, the atmospheric resistances (r_a, r_s), which are calculated using well-established formulations, often determine the dry deposition velocity, which is consistent with the observations for wind velocities less than or approximately equal to 4 m s^{-1}. However, because of the rather rough estimation of r_c, the results for specific agents should be seen more as examples of possible solutions than as actual results. Furthermore, for the continuous-release case, there are indications [29,62] that the dry deposition velocity onto water and snow surfaces should be treated as a decreasing function of the time from the start of release of the agent, the reason for this being desorption of a previously deposited agent. In future work, it would be of interest to investigate if the same also occurs for hazardous gases onto vegetated surfaces.

5.2. Dispersion models

While different types of models could be used to investigate and illustrate the effects of dry deposition on the concentration of hazardous gas clouds, and in particular the importance of the combined effect of dry deposition and release height as well as atmospheric stratification, they all have their particular advantages and disadvantages.

Two box-type dispersion models were used in this research because they permit explicit formulation of the dry deposition process and also for the advantage of comparison and to be able to identify and exclude possible simulation model peculiarities that could lead to erroneous conclusions. The box model type is described in the literature [18,41] and has been used for simulation of long-range transport of pollutants. However, since the gas concentration in box-type models is constant with height, the dry deposition flux may be underestimated for ground-level releases. Another drawback of the box-type model is that the aerodynamic resistance is calculated for a certain cloud thickness, in this study taken to be at a distance of 10 km, which may be an underestimation of v_d for distances below 10 km and an overestimation for distances larger than 10 km. The selection of horizontal and vertical dispersion parameters also involves choosing among several alternatives, with those used in this work being in accordance with Briggs [44].

A Lagrange model with Langevin formulation was therefore used in addition to the box models. This model has a more realistic gas concentration and wind profile than the box model. The relatively large turning of the wind direction in stable stratification (Fig. 8), which dilutes the gas, contributes to the difference between the results from the box and Lagrange models (Fig. 2a). Since the Lagrange model itself calculates the turbulent transfer, the aerodynamic resistance is near zero and there is no need to determine a reference height to compute r_a as when using the box model. However, the Lagrange model type itself has some disadvantages. For example, with a finite number of Lagrange particles, any calculated mean value of concentration depends on the shape and size of the volume in which the mean value is calculated. Conditional concentration mean-values can be determined using kernel estimation. The likelihood of error in such estimates approaches zero as the number of particles approaches infinity, but they do so quite slowly [49]. Thus, there is an uncertainty in the results in practice, stemming from for example, the number of particles. Other uncertainties may arise in connection to specific parameters. For example, in the case of the maximum concentration of the gas cloud, several maximum values appear as the cloud grows due to some randomness built into the model, making determination of the exact location of the maximum point difficult.

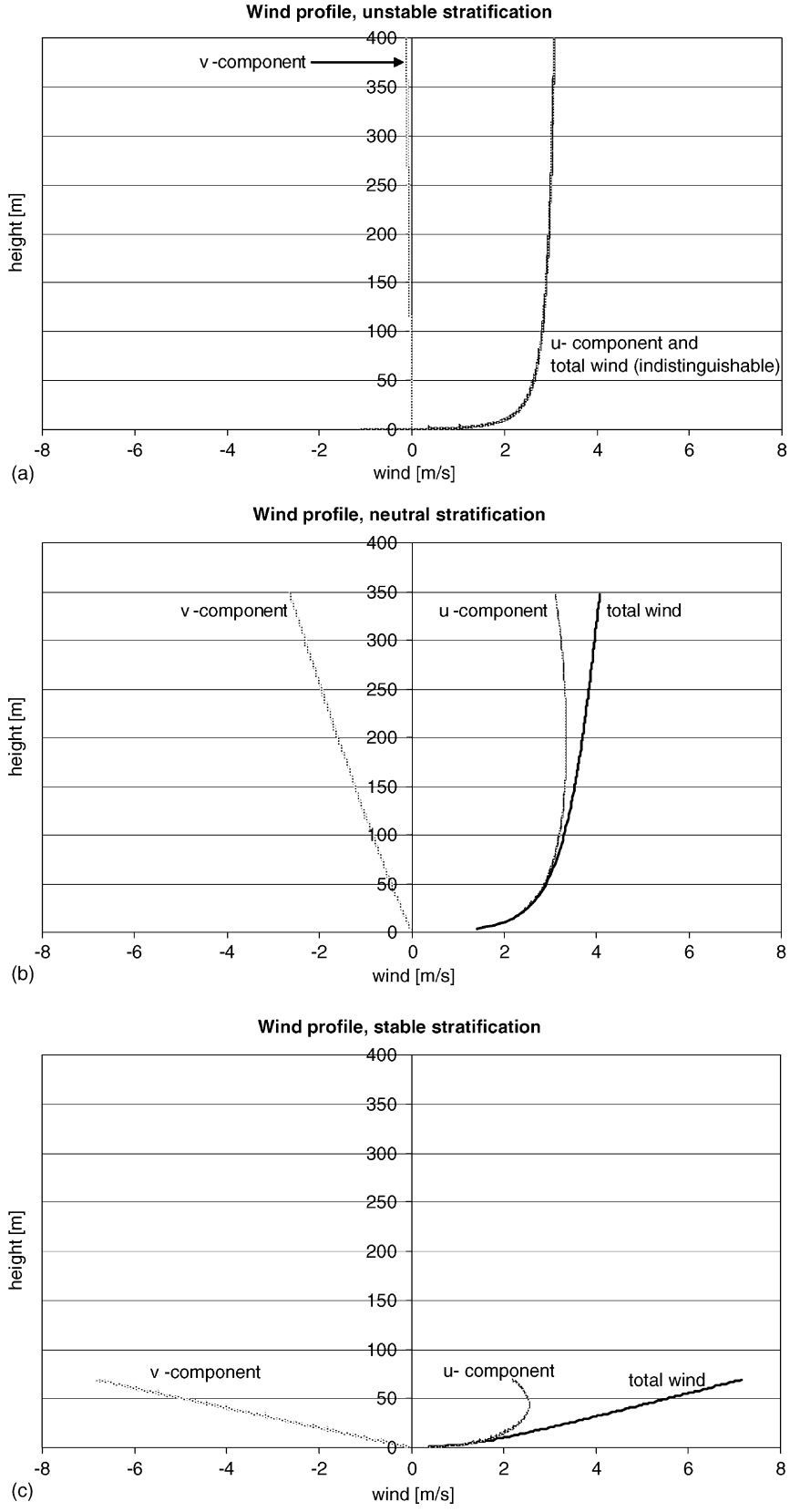

Fig. 8. The figure shows the wind profiles used in the Lagrange simulation for a wind speed of 2 m s^{-1} at 10 m height. Horizontal wind components are shown in the figure, as well as the total wind (solid curve); (a) shows the wind profile for unstable stratification, (b) for neutral stratification and (c) for stable stratification. For easier comparison, equal scales have been chosen in (a–c) though the PBL height is much lower for stable stratification. Notably, well below a height of 50 m the total wind speed for stable stratification exceeds that of both unstable and neutral stratification.

5.3. Influence of dry deposition on concentration of hazardous gas clouds for different kinds of releases

Using different types of models, a number of micrometeorological conditions were investigated for three different scenarios: a puff release at 58–68 m height, a puff release at ground level, and continuous release. The gas concentration was found to be reduced by dry deposition at all distances. Consistent with results presented by Hanna et al. [17], the degree of reduction was found to depend on v_d, atmospheric stability, wind speed and release height. Furthermore, for sources extending from zero height above the ground, the results indicate that the dry deposition process influences dispersion in such a way that neutral or even unstable stratification may cause the highest concentration level in hazardous gas clouds some distance away from the source. This is most probable for situations where there is a low wind speed and for substances, terrain and weather conditions that render a high dry deposition velocity. On the other hand, as the height of the source increases, or if the source is elevated, this effect of dry deposition decreases, and is possibly diminished for some weather conditions. The results for the different scenarios are briefly discussed below.

5.3.1. Puff source with extension to ground level

As expected and predicted by the different models, stable stratification will lead to the highest gas-cloud concentration if dry deposition is not considered for a given wind at any distance from the source (Fig. 2a). However, including the process of dry deposition in the dispersion simulation changes the picture. As can be seen in Figs. 3 and 4, the concentration curves for stable stratification start at a higher concentration level close to the source but cross the curves representing neutral stratification after some distance. Although the two fundamentally different models used, the box-type model and the Lagrange LEM model, predict different absolute concentration levels (as revealed in comparing Figs. 3 and 4), the results from both of the models show the same tendency and in fact predict that neutral stratification causes a higher ground-level concentration at some distance away from the source than does stable stratification.

However, the distance to the intersection point is predicted to be much shorter by the Lagrange model than the box model, approximately 30 km compared to about 70 km, respectively. This is mainly due to a relatively large change in the wind direction with increasing height in stable stratification (Fig. 8) which dilutes the gas concentration at ground level. Moreover, as presented in Tables 2–3 and Table 7, the tendency becomes stronger as the wind decreases. The tendency is also strengthened by increasing dry deposition, as could be deduced from the combined information in Figs. 1 and 3. This is more pronounced for sources with a delimited vertical extension in close proximity to the ground, as shown in Fig. 4.

Note that if the source is very close to the ground, Fig. 4b shows that the distance to the intersection point becomes considerably shorter, i.e. for a source height of 0–1 m the distance to the intersection point could be around 10 km for VX or even shorter while the corresponding distance for a more diffuse source that is 0–10 m above the ground could be in the range of 30–80 km. For most release scenarios with industrial chemicals the risk distance is less than 10 km, which means that there may be no intersection within the risk distance.

5.3.2. Elevated puff source release at 58–68 m

The effect of dry deposition is a small reduction in the concentration at all distances. Contrary to the ground-level release, the result is similar to the situation with no deposition (Figs. 5 and 2b). No intersecting of the curves occurs. A comparison between elevated release and ground-level release shows dry deposition to have a greater effect on a ground-level release, resulting in a lower concentration than for an elevated release some distance away from the source (Fig. 6a and b). This relation between the concentration curves, for releases extending to ground level and elevated releases, is opposite to the situation with no dry deposition (Fig. 6c).

5.3.3. Continuous source in contact with the ground

The effect of dry deposition for a continuous source in contact with the ground is similar to that found for the puff source at ground level, but the distances to the intersection points differ somewhat (Fig. 7). Thus, the continuous-source box-type model employed supports the tendencies observed in the results of the puff box-type and corresponding Lagrange LEM model simulations.

5.3.4. Half-value time and half-value distance

In agreement with the results by Hanna et al. [17], it can be seen (Tables 5 and 6) that the influence of dry deposition was predicted to be strongest when the source is close to and confined close to the ground, the stratification is stable, the wind speed is low and the dry deposition velocity high. Since low-height sources are typical of industrial chemical releases, this means that the concentration is predicted to be significantly reduced also for Cl_2, NH_3, or HF, although the intersection point may not be reached within the risk distance. However, as pointed out, the presented figures of half-value times/distances are strongly influenced by rather moderate changes in parameters such as wind speed, physical location and source extension. Note that the above factors identified as leading to the process of dry deposition having a strong influence on the cloud concentration are the same factors, which in certain combinations may cause a neutral, or even an unstable stratification to render the highest concentration of the hazardous gas cloud some distance away from the release.

5.4. Risk distance and human injury

The reduced hazardous-gas concentration due to dry deposition also reduces the risk distance for toxic gases, especially for ground-level releases and a low vertical extent of source height, e.g. heavy gases. The reduction in risk distance may

be even more pronounced than the reduction in concentration according to reported results [63–66] indicating that the toxic effect depends on $\int c^n \mathrm{d}t$, where $n \geq 1$, which may increase the effect of a concentration change. The intersecting of the concentration curves in Figs. 3, 4 and 7 can also be related to risk distance, and indicate the highest risk to exist at neutral or unstable concentration at some distance away from the source. This is important especially for toxic gases with risk distances greater than approx. 10 km, e.g. nerve agents. Consequently, with regard to the development of risk and alarm templates intended for use in any atmospheric stratification, many weather conditions should be considered as the dry deposition process can lead to different types of atmospheric stratification rendering the highest risk at some distance from the source. This especially applies to low risk levels that would be associated with longer risk distances.

5.5. Implications for aerosols

The effect of wind and terrain on dry deposition is different for aerosols and gases [60]. Thus, the results for gases cannot be assumed to fully apply to the case of hazardous aerosols (e.g. biological warfare agents). However, some similarities probably do exist. Clearly there is also a need to investigate the effects of dry deposition on consequences and risk areas after aerosol releases.

6. Conclusions

Two main conclusions can be drawn:

(a) Dry deposition may substantially reduce the concentration, risks and consequences following the release of a toxic gas, especially at long distances and for very stable stratification. This indicates that it is essential that the dry deposition process be carefully described and modeled in order to make more realistic calculations and estimations.

(b) A worst-case scenario for a release at ground level may not necessarily include the condition of stable stratification. Our findings indicate that instead, due to the effects of dry deposition, a neutral or even unstable stratification may lead to the highest toxic-gas concentration and longest risk distance. This appears to contradict what is normally believed and reflected in rules of thumb and handbooks.

Acknowledgements

The authors gratefully acknowledge the support of Dr. Per-Erik Johansson for his helpful comments and suggestions, and also wish to thank Ms. Kjerstin Granström and Ms. Åsa Lundvall for their assistance in preparing the manuscript.

Appendix A

In extending Eq. (10) to a model equation for a simple three-dimensional homogenous puff including dry deposition, Eq. (11), it should be noted that if $H = H(x)$, i.e. H varies in the down-wind direction, Eq. (11) is not a genuine solution to Eq. (8).

In order to get an idea of how close Eq. (11) approximates a solution to Eq. (8), let

$$H(x) = H_0 + \phi_z x \tag{A.1}$$

where ϕ_z is a vertical constant dispersion parameter

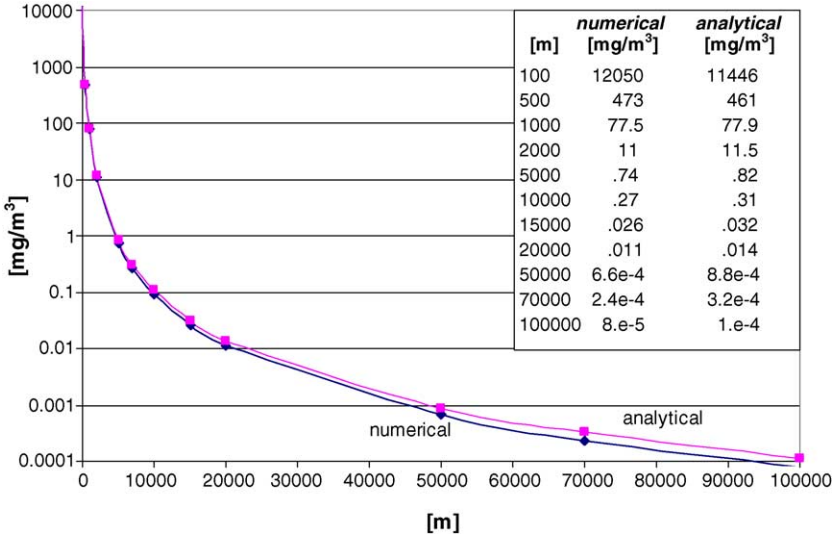

Fig. A.1. One plot (denoted "numerical") of a numerical solution to Eq. (A.2) multiplied by Π and another plot (denoted "analytical") of the concentration as given by Eq. (11). The values used for the plot are $C_0 = 100000\ \mathrm{mg/m^3}$, $u = 2\ \mathrm{m\,s^{-1}}$, $v_\mathrm{d} = 0.0059\ \mathrm{m\,s^{-1}}$, $L_0 = 10\ \mathrm{m}$, $S_0 = 10\ \mathrm{m}$, $H_0 = 10\ \mathrm{m}$ and Φ_x, Φ_y, and Φ_z with values recommended by Briggs [44] for stability class E [45,46].

Eq. (A.1), (9) in (8) results in:

$$\frac{\mathrm{d}}{\mathrm{d}x}(C(x)) = -\frac{(d+ex)}{(a+bx+cx^2)}C(x) \tag{A.2}$$

where the notations (A.3)–(A.7) below have been used.

$$a = uH_0L_0 \tag{A.3}$$

$$b = 2uH_0\phi_y + uL_0\phi_z \tag{A.4}$$

$$c = 2u\phi_y\phi_z \tag{A.5}$$

$$d = 2uH_0\phi_y + uL_0\phi_z + v_dL_0 \tag{A.6}$$

$$e = 4u\phi_y\phi_z + 2v_d\phi_y \tag{A.7}$$

where ϕ_x, ϕ_y are lateral and constant dispersion parameters.

Eq. (A.2), with the initial condition $C(0) = C_0$ could easily be solved numerically. For $\phi_z = 0$, the numerical solution to Eq. (A.2) shows identical results as Eq. (10). To be able to compare the solution to Eq. (A.2), i.e. $C(x)$, with the $\phi_z \neq 0$ puff model, Eq. (11), $C(x)$ is multiplied by $\frac{1}{(1+2\phi_x(x/S_0))} = \Pi$, thus imposing mass conservation while the cloud is symmetrically growing in the downwind direction. To illustrate the agreement, a plot of one numerical solution of Eq. (A.2) multiplied by Π is shown in Fig. A.1, where it could be compared with a plot of the corresponding analytical result derived from Eq. (11).

Thus, it can be expected that Eq. (11), considering formal reasons only, would yield a model useful for the analysis describing the concentration generated by a ground-level puff including the effect of dry deposition.

References

[1] G.A. Sehmel, Particle and gas dry deposition: A review, Atmos. Environ. 14 (1980) 983–1011.

[2] E. Karlsson, Theoretical model for dry deposition of nerve agents to snow and water surfaces, Proceedings of the 1993 ERDEC Scientific Conference on Chemical Defence Research, 16–19 November 1993. ERDEC-SP-024, pp-407–413, Edgewood Research Development and Engineering Centre, USA.

[3] J. Nikmo, J.P. Tuovinen, J. Kukkonen, I. Valkama, A Hybrid Plume Model For Local-Scale Dispersion, Publication of Air Quality No. 27, Finnish Meteorological Institute, 1997.

[4] L. Zhang, J.R. Brook, R. Vet, A revised parameterization for gaseous dry deposition in air-quality models, Atmos. Chem. Phys. 3 (2003) 2067–2082.

[5] M.L. Wesley, Parameterization of surface resistances to gaseous dry deposition in regional-scale numerical models, Atmos. Environ. 23 (1989) 1293–1304.

[6] V.M. Fthenakis, HGSYSTEM: a review, critique, and comparison with other models, J. Loss Prev. Proc. Ind. 12 (1999) 525–531.

[7] K. Riikonen, J. Kukkonen, J. Nikmo, A.L. Savolainen, A Model For Dispersion Of Hazardous Materials, NBC Defence 94, Research Centre of the Defence Forces, Finland, 1994, pp. 87–88.

[8] S. Fischer, R. Forsen, O. Herzberg, A. Jacobsson, B. Koch, P. Runn, L. Thaning, S. Winter, Toxic And Inflammable/Explosive Chemicals – A Swedish Manual For Risk Assessment, FOA-R-97-00490-990–SE (in Swedish), 1997.

[9] D.R. Blackmore, M.N. Herman, J.L. Woodward, Heavy gas dispersion models, J. Haz. Mat. 6 (1982) 107–128.

[10] S. Ott, An integral model for continuous HF release, Risoe-R-1293 (EN), 2001.

[11] L. D. Ermark, User's manual for SLAB: an atmospheric dispersion model for denser-than–air releases (draft, November version), Lawrence Livermore National Laboratory, Livermore, CA 94550, USA, 1999.

[12] T.O. Spicer, J.A. Havens, DEGADIS, Version 2.1, USEPA, Research Triangle Park, North Carolina, USA, 1989.

[13] C.G. Booij, The investigation into the spreading and dispersion of a heavy gas cloud by means of plant damages in the affected area, in: Proceedings of the 10th International Technical Meeting on Air Pollution Modelling and its Application, October 22–26, 1979, NATO Committee on the Challenge to Modern Society, 1979, pp. 655–662.

[14] M.P. Singh, S. Ghosh, Bhopal gas tragedy: model simulation of dispersion scenario, J. Haz. Mat. 17 (1987) 1–22.

[15] E. Karlsson, Indoor deposition reducing the effect of toxic gas clouds in ordinary buildings, J. Haz. Mat. 38 (1994) 313–327.

[16] E. Karlsson, U. Huber, Influence of desorption on the indoor concentration of toxic gases, J. Haz. Mat. 49 (1996) 15–27.

[17] S.R. Hanna, G.A. Briggs, R.P. Hosker Jr., Handbook on Atmospheric Diffusion, DOE/TIC-11223, USA 1982, p. 69.

[18] E. Karlsson, Long-range transport of biological agents, in: Siwert Nilsson, Bhoj Raj (Eds.), Some Model Calculations, Nordic Aerobiology, Almqvist & Wiksell International, Stockholm, Sweden, 1994, pp. 58–61.

[19] Chemical Weapons – Threat, Effects and Protection, FOI Briefing Book On no. 2, Swedish Defence Research Agency, 2002, pp. 64–69.

[20] NBC Analyses for Windows, Dos and Unix. Bruhn NewTech A/S, Sixth International Symposium on Protection against Chemical and Biological Warfare Agents, Stockholm Sweden 10–14 May, 1998 (Exhibition 150:16).

[21] E. Karlsson, E. Näslund, S.-E. Gryning, Comparision between experimental data and a Langevin particle dispersion model including dry deposition, in: Grying, Schiermeier (Eds.), Air Pollution and its Application XI, Plenum Press, New York, 1996, pp. 363–371.

[22] A.C. Chamberlain, Transport of gases from grass and grass-like surfaces, Proc. R. Soc. London A290 (1966) 236–265.

[23] J.A. Garland, The dry deposition of sulphur dioxide to land and water surfaces, Proc. R. Soc. London A354 (1977) 245–268.

[24] A.C. Chamberlain, Transport of Lycopodium spores and other small particles to rough surfaces, Proc. R. Soc. London A296 (1966) 45–70.

[25] M.L. Wesely, B.B. Hicks, Some factors that affect the deposition rates of sulfur dioxide and similar gases on vegetation, J. Air Pollut. Contr. Assoc. 27 (1977) 1110–1116.

[26] D. Fowler, Phil., Transfer to terrestrial surfaces, Trans. R. Soc. London B305 (1984) 281–297.

[27] J.W. Erisman, P. Addo, P. Wyers, Parameterization of surface resistance for the quantification of atmospheric deposition of acidifying pollutants and ozone, Atmos. Env. 28 (16) (1994) 2595–2607.

[28] Air Pollution Meteorology and Dispersion, Arya S.P., Oxford University Press, ISBN-0-19-507398-3, 1999.

[29] E. Karlsson, S. Nyholm, Dry deposition and desorption of toxic gases to and from snow surfaces, J. Haz. Mat. 60 (1998) 227–245.

[30] L. Zhang, J.R. Brook, R. Vet, A revised parameterization for gaseous dry deposition in air-quality models, Atmos. Chem. Phys. 3 (2003) 2067–2082.

[31] B.B. Hicks, D.D. Baldocchi, T.P. Meyers, R.P. Hosker, D.R. Matt, A preliminary multiple resistance routine for deriving dry deposition velocities from measured quantities, Water Air Soil Pollut. 36 (1987) 311–330.

[32] L. Zhang, M.D. Moran, P.A. Makar, J.R. Brook, S. Gong, Modeling gaseous dry deposition in AURAMS: a unified regional air-quality modeling system, Atmos. Env. 36 (2002) 537–560.

[33] M.L. Wesely, Parameterization of surface resistances to gaseous dry deposition in regional.scale numerical models, Atmos. Env. 23 (1989) 1293–1304.
[34] T.J. Bauer, R.L. Gibbs, V.A. Dahlgren, Software User's Manual for the Chemical/Biological Agent Vapor, Liquid and Solid Tracking (VLSTRACK) Computer Model, Version 3.0, Systems Research and Technology Department, Naval Surface Warfare Center, NSWCDD/TR-98/62, USA, 1998.
[35] R.I. Sykes et. al., PC-SCIPUFF Version 1.2PD, Technical Documentation, Titan Corporation, Research and Technology Division, Princeton, NJ, 1998.
[36] R. Lange, ADPIC – a three-dimensional particle-in-cell model for the dispersal of atmospheric pollutants and its comparison to regional tracer studies, J. App. Meteor. 17 (1978) 320–329.
[37] R. Lange, Transferability of the Three-Dimensional Air Quality Model Between Two Different Sites in Complex Terrain, J. Climate Appl. Meteorol. 28 (1989) 665–679.
[38] C.A. Sherman, A Mass-Consistent Model for Wind Fields over Complex Terrain, J. Appl. Meteorol. 17 (1978) 312–319.
[39] T.S. Sullivan, J.S. Ellis, C.S. Foster, K.T. Foster, R.L. Baskett, J.S. Nasstrom, W.W. Schalk III, Atmospheric release advisory capability: real-time modeling of airborne hazardous materials, Bull. Am. Meteorol. Soc. 74 (1993) 2343–2361.
[40] L. Robertson, J. Langner, M. Enghardt M, MATCH-Meso-scale atmospheric transport and chemistry modeling system, Basic transport model description and control experiments with ^{222}Rn, Swedish Meteorological and Hydrological Institute, RMK-70, Norrkoping, Sweden, 1996.
[41] R.A. Scriven, B.E.A. Fisher, The long range transport of airborne material and its removal by deposition and washout, Atmos. Env. 9 (1975) 49–58.
[42] S.R. Hanna, Review of atmospheric diffusion models for regulatory applications, WMO-No. 581, WMO, Geneva, Switzerland, 1982, pp. 19–20.
[43] K. Nodop, EUR 17346 – ETEX Symposium on Long-Range Atmospheric Transport, Model Verification and Emergency Response, 13-16 May 1997. Vienna (Austria), Proceedings, Office for Official Publications of the European Communities, ISBN 92-828-0669-3, Luxembourg, 1997.
[44] G.A. Briggs, Diffusion Estimation for Small Emissions, ATDL Contribution File No. 79, ADTL/NOAA, P.O. Box E, Oak Ridge, TN, 37830, 1973, p. 59.
[45] F. Pasquill, Estimation of the dispersion of windborne material, Meteorol. Mag. 90 (1961) 33–49.
[46] D.B. Turner, Workbook of Atmospheric Dispersion Estimates, second ed., Lewis Pub., CRC Press, Boca Raton, FL, 1970.
[47] G.I. Taylor, Diffusion by continuous movements, Proc. London Math. Soc. 20 (1921) 196–212.
[48] K.H. Im, P.M. Chung, AIChE J. 29 (3) (1983) 498–505.
[49] S.B. Pope, Turbulent Flows, Cambridge University Press, Cambridge U.K, 2000, pp. 483–494.
[50] P. Langevin, Sur la théorie du mouvement Brownien, Comptes Rendus Acad. Sci., Paris 146 (1908) 530–533.
[51] E. Näslund, C. Rodean, J.A. Nasstrom, A comparision between two stochastic diffusion models in a complex three-dimensional flow, Bound. Lay. Meteorol. 67 (1994) 369–384.
[52] H.C. Rodean, Notes on the Langevin Model for Turbulent Diffusion of Marked Particles, UCRL-ID-115869, Lawrence Livermore National Laboratory, Livermore, CA, 1994.
[53] C.C. Lin, W.H. Reid, Turbulent Flow, Handbuch der Physics, VIII/2, Springer Verlag, Berlin, 1962, pp. 438–523.
[54] J.D. Wilson, G.W. Thurtell, G.E. Kidd, Numerical simulation of particle trajectories in inhomogeneous turbulence II: Systems with variable turbulence velocity scale, Bound. Lay. Meteorol. 21 (1981) 423–441.
[55] J.H. Baerentsen, R. Berkowizc, Monte Carlo simulation of plume dispersion in the convective boundary layer, Atmos. Env. 18 (1984) 701–712.
[56] S.S. Zilitinkevich, D.V. Mironov, A multi-limit formulation for the equilibrium depth of a stably stratified boundary layer, Bound. Lay. Meteorol. 81 (1996) 325–351.
[57] F. Reif, Fundamentals of Statistical and Thermal Physics, McGraw-Hill, 1965, pp. 269–273.
[58] B.A. Boughton, J.M. Delaurentis, W.E. Dunn, A stochastic model of particle dispersion in the atmosphere, Bound. Lay. Meteorol. 40 (1987) 147–163.
[59] J.D. Wilson, F.J. Ferrandino, G.W. Thurtell, A relationship between deposition velocity and trajectory reflection probability for use in stochastic Lagrangian dispersion models, Agr. For. Meteorol. 47 (1989) 139–154.
[60] L. Zhang, S. Gong, J. Padro, L. Barrie, A size-segregated particle dry deposition scheme for an atmospheric aerosol module, Atmos. Env. 35 (2001) 549–560.
[61] W.J. Lyman, W.F. Reehl, D.H. Rosenblatt, Handbook of Chemical Property Estimation Methods, American Chemical Society, Washington, DC, 1990, Chapter 17.
[62] R.C. Bales, M.P. Valdez, G.A. Dawson, Gaseous deposition on snow: 2 Physical-chemical model for SO_2 deposition, J. Geophys. Res. 92 (1987) 9789.
[63] D.J. Finney, Probit Analysis, third ed., Cambridge University Press, Cambridge, 1971.
[64] R.J. Mioduszewski, J.H. Manthei, R.A. Way, D.C. Burnett, B.P. Gaviola, W.T. Muse Jr., J.S. Anthony, H.D. Durst, D.R. Sommerville, R.B. Crosier, S.A. Thomson, C.L. Crouse, ECBC low level operational toxicology program: Phase 1 - Inhalation toxicity of Sarin vapour in rats as a function of exposure concentration and duration, ECBC-TR-183, U.S. Army Edgewood Chemical Biological Centre, Aberdeen Proving Ground, MD, 2001.
[65] TNO, Methods for the Determination of Possible Damage: to people and objects resulting from releases of hazardous materials, Re CPR-16E ("The Green Book") Committee for the Prevention of Disaters caused by Dangerous Substances, Voorburg, First ed. CIP-data of the Royal Library, Hague, 1992.
[66] R.W. Bide, D.J. Risk, GB Toxicity in Mice Exposed for 20 to 720 Min., Defence R&D Canada (DRDC), TR-2002-031, Suffield, Canada, 2002.